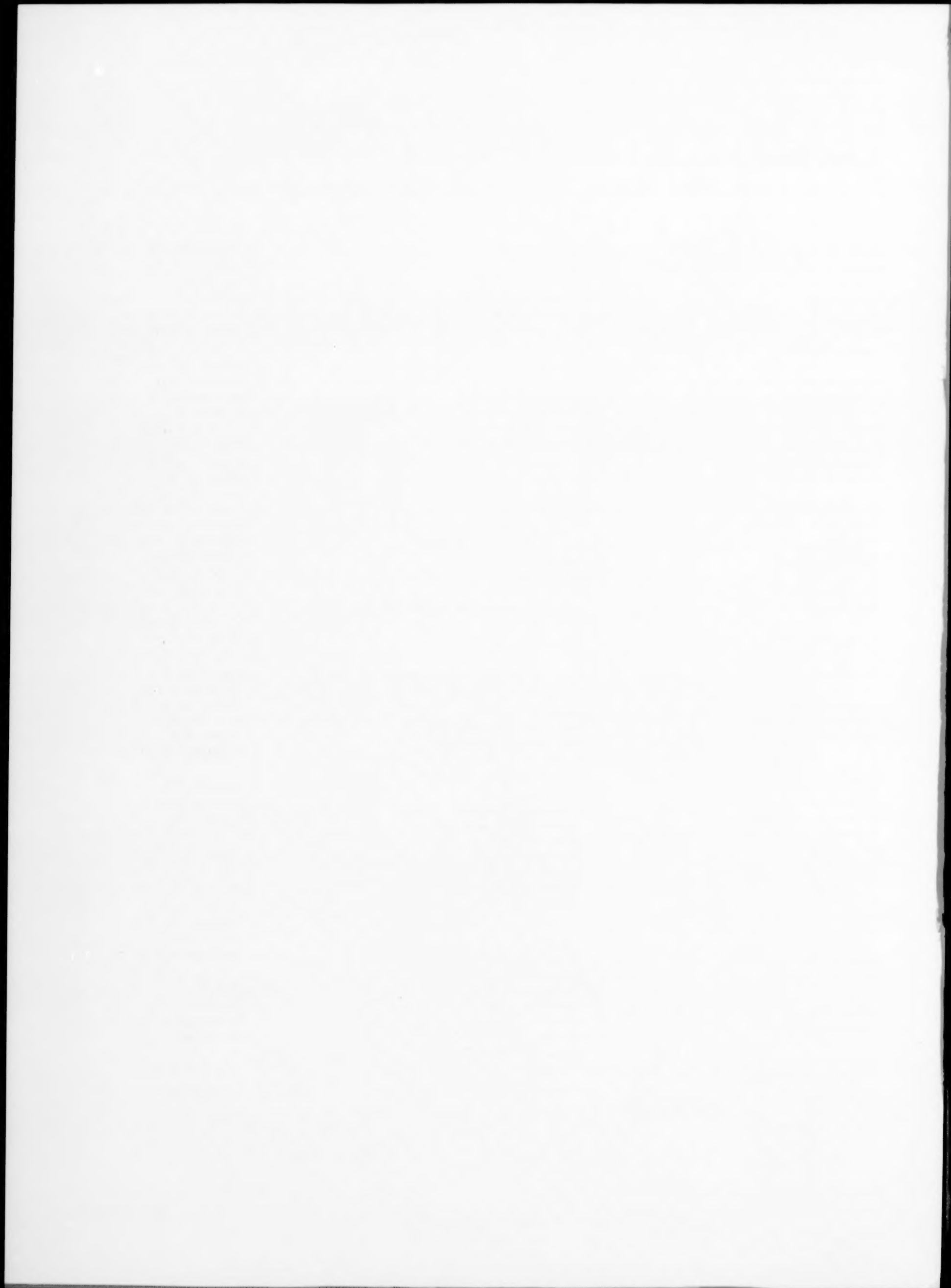


## Author Index of Volume 176

- Abiko, K., 363  
 Adachi, Y., 271  
 Ai, S. H., 393  
 Aoki, M., 19  
 Argon, A. S., 79, 111  
 Arimitsu, Y., 271  
 Aust, K. T., 329  
  
 Birnbaum, H. K., 191  
 Booth, A. S., 91  
  
 Carlsson, A. E., 255  
 Choi, P. K., 231  
 Chou, Y. T., 421  
 Cohen, R. E., 79  
  
 Dickinson, J. T., 411  
 Doyama, M., 277  
 Dunn, M. L., 349  
 Duxbury, P. M., 25  
  
 Enoki, M., 289  
 Erb, U., 329  
  
 Fields, B. A., 51  
 Fu, C. L., 431  
 Fujita, S., 121  
  
 George, A., 99  
 Golubeva, N. G., 309  
 Goto, K., 357  
  
 Harmer, M. P., 421  
 Hatta, H., 165  
 Haze, T., 385  
 Higashi, K., 181, 461  
 Higashida, K., 147, 203  
 Hirsch, P. B., 91  
 Hoagland, R. G., 219  
 Hockey, B. J., 51  
 Horton, J. A., 431  
 Hsia, K. J., 111, 155  
 Hyodo, S., 231  
  
 Ishikawa, T., 385, 397  
 Itaba, H., 283  
  
 Jones, R. H., 211  
 Josefowicz, J. Y., 405  
  
 Kagawa, Y., 165, 357, 379  
 Katakura, S., 417  
 Kikuchi, A., 171  
  
 Kim, B. N., 371  
 Kim, S. G., 25  
 Kimura, A., 425  
 Kirchner, H. O. K., 177  
 Kishi, T., 289, 371  
 Kitagawa, H., 263  
 Kitajima, K., 249  
 Kodama, Y., 231  
 Kogo, Y., 165  
 Koide, M., 171  
 Koizumi, H., 231, 417  
 Koya, A., 425  
 Kulawansa, D. M., 411  
  
 Langer, J. S., 33, 317  
 Langford, S. C., 411  
 Leath, P. L., 25  
 Lee, S., 127, 335  
 Li, Y. Z., 421  
 Lim, L. C., 439  
 Liu, C., 363  
 Liu, Y., 219  
 Loyola de Oliveira, M. A., 99, 139  
 Lu, H. H., 439  
 Lung, C. W., 299  
  
 Mabuchi, M., 461  
 Maeda, K., 121, 225  
 Maekawa, K., 283  
 Maksimov, I. L., 309, 321  
 Maksimova, G. M., 309  
 Marrow, T. J., 455  
 Masuda-Jindo, K., 225, 255  
 Matsunaga, K., 147  
 Metrikin, V. S., 309  
 Michot, G., 99, 139, 177  
 Misawa, T., 425  
 Morimura, T., 425  
 Mower, T. M., 79  
 Mukai, T., 181  
 Mura, T., 61  
  
 Nagumo, M., 171  
 Nakamura, Y., 411  
 Nakanishi, H., 33, 317  
 Nakatani, A., 263  
 Narita, N., 121, 147, 203  
 Neumann, P., 9  
 Nishioka, H., 121, 271  
 Nietzsche, V. R., 155  
  
 Ozawa, S., 283  
  
 Palumbo, G., 329  
 Pettifor, D. G., 19  
 Pope, D. P., 405  
 Puls, M. P., 237  
  
 Roberts, S. G., 91, 455  
  
 Sagat, S., 237  
 Sakuma, T., 447  
 Sasijima, Y., 283  
 Shi, S. Q., 237  
 Shibutani, Y., 263  
 Shiga, T., 203  
 Shimamura, S., 303  
 Shindo, Y., 471  
 Shiue, S.-T., 127  
 Simonen, E. P., 211  
 Smirnova, V. N., 309  
 Smith, M. A., 405  
 Sofronis, P., 191  
 Suzuki, T., 417  
 Svirina, J. V., 309, 321  
  
 Taguchi, Y. H., 295  
 Tajima, J., 271  
 Takai, T., 271  
 Tanaka, H., 283, 341  
 Tanimura, S., 181  
 Tanino, M., 363  
 Taya, M., 349  
 Thomson, R., 1, 255  
 Tsurekawa, S., 341  
  
 Ueda, S., 471  
 Umezawa, O., 397  
 Utoh, Y., 289  
  
 Vehoff, H., 71  
  
 Wang, Z. G., 393  
 Watanabe, T., 39  
 Watanabe, Y., 411  
 Weertman, J., 131  
 Wiederhorn, S. M., 51  
  
 Yagi, T., 171  
 Yoo, M. H., 431  
 Yoshinaga, H., 341  
 Yoshizawa, Y., 447  
  
 Zheng, Y. S., 393  
 Zhou, S. J., 255



## Subject Index of Volume 176

### Alloys

- acoustic emission associated with the fracture of Al and Al alloy embrittled by liquid gallium, 231
- crack initiation criterion at notches in Zr-2.5Nb alloys, 237
- crack-impurity interactions and their role in the embrittlement of Fe alloy crystals charged with light elements, 203
- experimental investigation of cavitation fracture at very high strain rates in superplastic aluminium alloy matrix composites, 461
- influence of the magnesium concentration on the relationship between fracture mechanism and strain rate in high purity Al-Mg alloys, 181
- phenomenological aspects of fatigue life and fatigue crack initiation in high strength alloys at cryogenic temperature, 397
- role of chromium in the intergranular fracture of high purity Fe-P-Cr alloys with small amounts of carbon, 363

### Alumina

- high-temperature deformation and cavitation in fine-grained alumina, 447
- toughening mechanisms in the high temperature fracture of high purity alumina, 455

### Aluminium

- acoustic emission associated with the fracture of Al and Al alloy embrittled by liquid gallium, 231
- crack-tip dislocations and fracture behavior in Ni<sub>3</sub>Al and Ni<sub>3</sub>Si, 431
- estimation of fracture resistance of Al<sub>2</sub>O<sub>3</sub> polycrystals from single-crystal values, 371
- experimental investigation of cavitation fracture at very high strain rates in superplastic aluminium alloy matrix composites, 461
- influence of the magnesium concentration on the relationship between fracture mechanism and strain rate in high purity Al-Mg alloys, 181

### Atomic force microscopy

- atomic force microscopy observations of iron-sapphire fracture surfaces, 405

### Atomic theory

- atomic theory of fracture of crystalline materials: cleavage and dislocation emission criteria, 255

### Atomistic simulations

- directional bonding in atomistic simulations, 19

### Bonding

- directional bonding in atomistic simulations, 19

### Brittle-to-ductile transition

- modelling of dislocation mobility controlled brittle-to-ductile transition, 155

### Carbon

- brittle fracture initiation in low carbon steels at ductile-brittle transition temperature region, 171
- fracture of silicon nitride and silicon carbide at elevated temperatures, 51

### Cavitation

- high-temperature deformation and cavitation in fine-grained alumina, 447

### Ceramics

- crack-fiber interaction and interfacial failure models in fiber-reinforced ceramics, 357
- quantitative analysis of closure stress-crack separation curve in grain bridge toughening of polycrystalline ceramics, 379
- stochastic microfracture process of ceramics, 289

### Chlorine

- crack propagation velocity in NaCl single crystals, 417

### Chromium

- role of chromium in the intergranular fracture of high purity Fe-P-Cr alloys with small amounts of carbon, 363

### Cleavage

- atomic theory of fracture of crystalline materials: cleavage and dislocation emission criteria, 255
- experimental study of the mechanisms of brittle-to-ductile transition of cleavage fracture in Si single crystals, 111
- significance of fracture facet size in cleavage fracture process of welded joints, 385

### Composites

- experimental investigation of cavitation fracture at very high strain rates in superplastic aluminium alloy matrix composites, 461
- modeling of thermal cycling creep damage of short fiber metal matrix composites, 349

### Computer simulation

- atomistic consideration and computer simulation of the initiation and the process of crack propagation, 271

### Conduction

- thermomechanical fracture instabilities in the current-carrying state of conducting media, 321

### Corrosion

- early stages in the development of stress corrosion cracks, 211

### Cracking

- a simple model for crack propagation, 317
- a theory on fatigue crack initiation, 65
- analysis of crack-dislocation interaction: crack closure, crack opening, 139
- asymptotic dislocation density fields for cracks in an elastic, perfectly plastic solid, 131
- atomistic consideration and computer simulation of the initiation and the process of crack propagation, 271
- brittle-to-ductile transition studied by constant-rate indentation cracking, 121
- crack initiation criterion at notches in Zr-2.5Nb alloys, 237
- crack propagation velocity in NaCl single crystals, 417
- crack-fiber interaction and interfacial failure models in fiber-reinforced ceramics, 357
- crack-impurity interactions and their role in the embrittlement of Fe alloy crystals charged with light elements, 203
- crack-tip dislocations and fracture behavior in Ni<sub>3</sub>Al and Ni<sub>3</sub>Si, 431
- dislocation loops at crack tips: control and analysis of sources in silicon, 99
- early stages in the development of stress corrosion cracks, 211
- effect of dislocation activities on crack extension in ionic crystals, 147



- effect of dislocation substructure of crack tip on near fatigue threshold in dual-phase steels, 393
- environmental effects of crack tip processes at the atomic level, 219
- general solution of screw dislocations near an interfacial crack, 335
- interface control for resistance to intergranular cracking, 329
- molecular dynamics study of crack processes associated with dislocation nucleated at the tip, 263
- phenomenological aspects of fatigue life and fatigue crack initiation in high strength alloys at cryogenic temperature, 397
- quantitative analysis of closure stress-crack separation curve in grain bridge toughening of polycrystalline ceramics, 379
- dislocation-free zone model of mode III fracture: the effect of crack bluntness, 127
- theory of non-isothermal crack propagation in plastic and viscous-plastic materials, 309
- weight functions for short cracks, 177
- Creep**
  - modeling of thermal cycling creep damage of short fiber metal matrix composites, 349
- Crystals**
  - atomic theory of fracture of crystalline materials: cleavage and dislocation emission criteria, 255
  - computer experiments of fracture process of two-dimensional Henley-Elser type quasicrystals, 283
  - crack propagation velocity in NaCl single crystals, 417
  - crack-impurity interactions and their role in the embrittlement of Fe alloy crystals charged with light elements, 203
  - dislocation activity and brittle-ductile transitions in single crystals, 91
  - effect of dislocation activities on crack extension in ionic crystals, 147
  - estimation of fracture resistance of  $Al_2O_3$  polycrystals from single-crystal values, 371
  - experimental study of the mechanisms of brittle-to-ductile transition of cleavage fracture in Si single crystals, 111
  - quantitative analysis of closure stress-crack separation curve in grain bridge toughening of polycrystalline ceramics, 379
  - simulation of plastic deformation and fracture of small crystals, 277
  - the impact of grain boundary character distribution upon fracture in polycrystals, 39
- Damage**
  - modeling of thermal cycling creep damage of short fiber metal matrix composites, 349
- Deformation**
  - high-temperature deformation and cavitation in fine-grained alumina, 447
  - simulation of plastic deformation and fracture of small crystals, 277
- Dislocation**
  - analysis of crack-dislocation interaction: crack closure, crack opening, 139
  - asymptotic dislocation density fields for cracks in an elastic, perfectly plastic solid, 131
  - atomic theory of fracture of crystalline materials: cleavage and dislocation emission criteria, 255
  - crack-tip dislocations and fracture behavior in  $Ni_3Al$  and  $Ni_3Si$ , 431
  - dislocation activity and brittle-ductile transitions in single crystals, 91
  - dislocation loops at crack tips: control and analysis of sources in silicon, 99
  - effect of dislocation activities on crack extension in ionic crystals, 147
  - effect of dislocation substructure of crack tip on near fatigue threshold in dual-phase steels, 393
  - general solution of screw dislocations near an interfacial crack, 335
  - modelling of dislocation mobility controlled brittle-to-ductile transition, 155
  - molecular dynamics study of crack processes associated with dislocation nucleated at the tip, 263
  - dislocation-free zone model of mode III fracture: the effect of crack bluntness, 127
- Ductility**
  - dynamic grain growth and ductility enhancement at intermediate temperature, 439
- Earthquakes**
  - dynamics of earthquakes and fracture, 33
- Elasticity**
  - asymptotic dislocation density fields for cracks in an elastic, perfectly plastic solid, 131
- Embrittlement**
  - brittle fracture initiation in low carbon steels at ductile-brittle transition temperature region, 171
  - brittle-to-ductile transition studied by constant-rate indentation cracking, 121
  - crack-impurity interactions and their role in the embrittlement of Fe alloy crystals charged with light elements, 203
  - dislocation activity and brittle-ductile transitions in single crystals, 91
  - embrittlement due to gaseous and liquid environments, 9
  - energetics and model simulation of impact fracture of brittle solids, 303
- Emissions**
  - acoustic emission associated with the fracture of Al and Al alloy embrittled by liquid gallium, 231
  - atomic theory of fracture of crystalline materials: cleavage and dislocation emission criteria, 255
- Fracture**
  - crack-tip dislocations and fracture behavior in  $Ni_3Al$  and  $Ni_3Si$ , 431
- Failure**
  - crack-fiber interaction and interfacial failure models in fiber-reinforced ceramics, 357
- Fatigue**
  - effect of dislocation substructure of crack tip on near fatigue threshold in dual-phase steels, 393
  - phenomenological aspects of fatigue life and fatigue crack initiation in high strength alloys at cryogenic temperature, 397
- Fibres**
  - crack-fiber interaction and interfacial failure models in fiber-reinforced ceramics, 357
  - modeling of thermal cycling creep damage of short fiber metal matrix composites, 349
  - singular stresses of glass fiber reinforced plastics with a broken layer at low temperatures, 471
- Flaws**
  - observation of fracture features in fused quartz with laser-induced internal flaws, 421
- Fracture**
  - a theory on fatigue crack initiation, 65
  - acoustic emission associated with the fracture of Al and Al alloy embrittled by liquid gallium, 231

- atomic force microscopy observations of iron-sapphire fracture surfaces, 405
  - atomic theory of fracture of crystalline materials: cleavage and dislocation emission criteria, 255
  - brittle fracture initiation in low carbon steels at ductile-brittle transition temperature region, 171
  - chemical environment effect on indentation-induced fracture of silicon, 225
  - computer experiments of fracture process of two-dimensional Henley-Elser type quasicrystals, 283
  - dynamical modelling of fracture propagation, 295
  - dynamics of earthquakes and fracture, 33
  - energetics and model simulation of impact fracture of brittle solids, 303
  - estimation of fracture resistance of  $\text{Al}_2\text{O}_3$  polycrystals from single-crystal values, 371
  - experimental investigation of cavitation fracture at very high strain rates in superplastic aluminium alloy matrix composites, 461
  - experimental study of the mechanisms of brittle-to-ductile transition of cleavage fracture in Si single crystals, 111
  - fracture of silicon nitride and silicon carbide at elevated temperatures, 51
  - high temperature fracture, 71
  - hydrogen enhanced localized plasticity—a mechanism for hydrogen-related fracture, 191
  - influence of the magnesium concentration on the relationship between fracture mechanism and strain rate in high purity Al-Mg alloys, 181
  - modelling of hydrogen-induced fracture in iron, 249
  - multirange fractal description of fractured surfaces, 299
  - nanometer-scale observations of metallic glass fracture surfaces, 411
  - observation of fracture features in fused quartz with laser-induced internal flaws, 421
  - role of chromium in the intergranular fracture of high purity Fe-P-Cr alloys with small amounts of carbon, 363
  - significance of fracture facet size in cleavage fracture process of welded joints, 385
  - simulation of plastic deformation and fracture of small crystals, 277
  - size effect and statistics of fracture in random materials, 25
  - stochastic microfracture process of ceramics, 289
  - the dislocation-free zone model of III fracture: the effect of crack bluntness, 127
  - the impact of grain boundary character distribution upon fracture in polycrystals, 39
  - thermomechanical fracture instabilities in the current-carrying state of conducting media, 321
  - toughening mechanisms in the high temperature fracture of high purity alumina, 455
- Gallium**
- acoustic emission associated with the fracture of Al and Al alloy embrittled by liquid gallium, 231
- Glass**
- nanometer-scale observations of metallic glass fracture surfaces, 411
  - singular stresses of glass fibre reinforced plastics with a broken layer at low temperatures, 471
- Grain boundary character distribution**
- the impact of grain boundary character distribution upon fracture in polycrystals, 39
- Grain boundary structure**
- grain boundary structure, energy and strength in molybdenum, 341
- Grain bridge toughening**
- quantitative analysis of closure stress-crack separation curve in grain bridge toughening of polycrystalline ceramics, 379
- Grain growth**
- dynamic grain growth and ductility enhancement at intermediate temperature, 439
- Henley-Elser quasicrystals**
- computer experiments of fracture process of two-dimensional Henley-Elser type quasicrystals, 283
- Hydrogen**
- hydrogen enhanced localized plasticity—a mechanism for hydrogen-related fracture, 191
  - modelling of hydrogen-induced fracture in iron, 249
- Impact properties**
- impact properties of intermetallic compounds, 425
- Impurities**
- crack-impurity interactions and their role in the embrittlement of Fe alloy crystals charged with light elements, 203
- Indentation**
- brittle-to-ductile transition studied by constant-rate indentation cracking, 121
- Interfaces**
- general solution of screw dislocations near an interfacial crack, 335
  - interface control for resistance to intergranular cracking, 329
- Intermetallics**
- impact properties of intermetallic compounds, 425
- Iron**
- atomic force microscopy observations of iron-sapphire fracture surfaces, 405
  - crack-impurity interactions and their role in the embrittlement of Fe alloy crystals charged with light elements, 203
  - modelling of hydrogen-induced fracture in iron, 249
  - role of chromium in the intergranular fracture of high purity Fe-P-Cr alloys with small amounts of carbon, 363
- Lasers**
- observation of fracture features in fused quartz with laser-induced internal flaws, 421
- Magnesium**
- influence of the magnesium concentration on the relationship between fracture mechanism and strain rate in high purity Al-Mg alloys, 181
- Metallics**
- nanometer-scale observations of metallic glass fracture surfaces, 411
- Molybdenum**
- grain boundary structure, energy and strength in molybdenum, 341
- Nickel**
- crack-tip dislocations and fracture behavior in  $\text{Ni}_3\text{Al}$  and  $\text{Ni}_3\text{Si}$ , 431
- Niobium**
- crack initiation criterion at notches in Zr-2.5Nb alloys, 237
- Nitrogen**
- fracture of silicon nitride and silicon carbide at elevated temperatures, 51
- Non-isothermal propagation**
- theory of non-isothermal crack propagation in plastic and viscous-plastic materials, 309
- Nucleation**
- molecular dynamics study of crack processes associated with dislocation nucleated at the tip, 261



**Oxygen**

- estimation of fracture resistance of  $\text{Al}_2\text{O}_3$  polycrystals from single-crystal values, 371

**Phosphorus**

- role of chromium in the intergranular fracture of high purity Fe-P-Cr alloys with small amounts of carbon, 363

**Plasticity**

- asymptotic dislocation density fields for cracks in an elastic, perfectly plastic solid, 131
- experimental investigation of cavitation fracture at very high strain rates in superplastic aluminium alloy matrix composites, 461
- hydrogen enhanced localized plasticity—a mechanism for hydrogen-related fracture, 191
- simulation of plastic deformation and fracture of small crystals, 277
- singular stresses of glass fibre reinforced plastics with a broken layer at low temperatures, 471
- theory of non-isothermal crack propagation in plastic and viscous-plastic materials, 309

**Polymers**

- mechanisms of toughening brittle polymers, 79

**Propagation**

- crack propagation velocity in NaCl single crystals, 417

**Quartz**

- observation of fracture features in fused quartz with laser-induced internal flaws, 421

**Resistance**

- interface control for resistance to intergranular cracking, 329

**Sapphire**

- atomic force microscopy observations of iron-sapphire fracture surfaces, 405

**Shielding**

- the experimental verification of the shielding effect in zirconia, 165

**Silicon**

- chemical environment effect on indentation-induced fracture of silicon, 225
- crack-tip dislocations and fracture behavior in  $\text{Ni}_3\text{Al}$  and  $\text{Ni}_3\text{Si}$ , 431

- dislocation loops at crack tips: control and analysis of sources in silicon, 99

- experimental study of the mechanisms of brittle-to-ductile transition of cleavage fracture in Si single crystals, 111

- fracture of silicon nitride and silicon carbide at elevated temperatures, 51

**Sodium**

- crack propagation velocity in NaCl single crystals, 417

**Steels**

- brittle fracture initiation in low carbon steels at ductile-brittle transition temperature region, 171

- effect of dislocation substructure of crack tip on near fatigue threshold in dual-phase steels, 393

**Strain**

- experimental investigation of cavitation fracture at very high strain rates in superplastic aluminium alloy matrix composites, 461

- influence of the magnesium concentration on the relationship between fracture mechanism and strain rate in high purity Al-Mg alloys, 181

**Stress**

- early stages in the development of stress corrosion cracks, 211

- quantitative analysis of closure stress-crack separation curve in grain bridge toughening of polycrystalline ceramics, 379

- singular stresses of glass fibre reinforced plastics with a broken layer at low temperatures, 471

**Toughening**

- toughening mechanisms in the high temperature fracture of high purity alumina, 455

**Viscosity**

- theory of non-isothermal crack propagation in plastic and viscous-plastic materials, 309

**Welding**

- significance of fracture facet size in cleavage fracture process of welded joints, 385

**Zirconium**

- crack initiation criterion at notches in Zr-2.5b alloys, 237

- the experimental verification of the shielding effect in zirconia, 165

